

# Joint Source-Environment Adaptation for Deep Learning-Based Underwater Acoustic Source Ranging

Dariusz Kari

University of Illinois Urbana-Champaign  
Urbana, IL, USA  
dkari2@illinois.edu

Andrew C. Singer

Stony Brook University  
Stony Brook, NY, USA  
andrew.c.singer@stonybrook.edu

**Abstract**—In this paper, we propose a method to adapt a pre-trained deep-learning-based model for underwater acoustic localization to a new environment. We use unsupervised domain adaptation to improve the generalization performance of the model, i.e., using an unsupervised loss, fine-tune the pre-trained network parameters without access to any labels of the target environment or any data used to pre-train the model. This method improves the pre-trained model prediction by coupling that with an almost independent estimation based on the received signal energy (that depends on the source). We show the effectiveness of this approach on Bellhop generated data in an environment similar to that of the SWellEx-96 experiment contaminated with real ocean noise from the KAM11 experiment.

**Index Terms**—underwater acoustic localization, domain adaptation, information maximization, source hypothesis transfer

## I. INTRODUCTION

Despite the success of deep learning (DL)-based underwater acoustic (UWA) localization algorithms [1]–[3], their applications remain limited due to poor generalization in mismatched environments [2], [4]. Domain adaptation (DA) methods can mitigate small mismatches between testing and training datasets by aligning their statistics [5], but these approaches require access to training data. However, with the growing adoption of decentralized processing [6]–[8], training data will not always be available due to the communication cost of transferring large datasets between low-power underwater devices or due to security or privacy issues. Therefore, this paper seeks to improve the generalization performance of DL-based UWA localization models via *source-free* DA [9].

In an effort to provide a more robust solution than matched field processing (MFP) [10], [11], Chen and Schmidt [2] propose a model-based convolutional neural network (CNN), which outperforms MFP in the presence of depth mismatch. To generate the training dataset, the authors use OASES [12] with the sound speed profile set according to the values measured in the real experiment. While a reasonable way to generate more realistic training data, this method does not consider the parameter shift between the synthetic training and the real testing environments. Moreover, it assumes a prior

knowledge of the parameters of the test environment, which is rarely available. This motivates further improvement using an adaptation mechanism.

The environmental mismatch problem is known in the machine learning literature as domain shift [13] and there are different approaches to its solution, including domain adaptation or domain generalization [9], [13], transfer learning [14], [15], and data augmentation [16]. While data augmentation and transfer learning have been studied for some cases in underwater acoustic localization [14], [17], DA remains mainly unexplored, with sparse studies like [4] and [18].

Whenever accessible, DA can leverage training data to learn the domain shift. Nonetheless, source-free DA [9] is still possible by inferring some useful statistics (features) of the training set from the pre-trained model. Note that not only can source-free DA respect the privacy in distributed settings, but also it can prevent the communication cost tied to large data-set transfer in a challenging underwater environment.

As a source-free DA method, source hypothesis transfer (SHOT) [9] assumes that the DL-based model consists of a domain-specific feature extractor and a domain-invariant classifier (hypothesis). During the inference, while freezing the classifier, SHOT fine-tunes the feature extractor to produce confident outputs and prevents it from a degenerated solution by using an information maximization loss [9] that promotes diverse output labels. While this procedure is useful for one-hot coded labels, it is not as effective for cases where labels are not equidistant, e.g., for localization.

Although localization naturally fits into a regression paradigm, regression in its standard form only outputs a point estimate, while a classification model provides a probability mass function (PMF). Hence, we use a classification model to obtain the model uncertainty from the output PMF, e.g., a unimodal PMF implies the model is more certain about its prediction compared to the case of a multimodal PMF. In addition, by using a metric-inspired label softening to preserve distances between different classes, we make the classification model more amenable to the localization problem.

Figure 1 shows an example output of a pre-trained classification model under environmental mismatch, where the largest

This work has been supported by the Office of Naval Research (ONR) under grant N00014-19-1-2662.

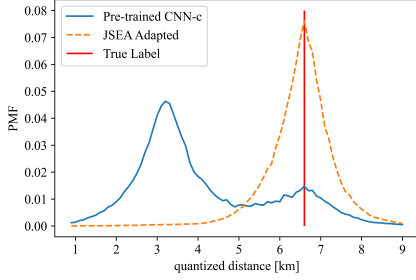


Fig. 1: An example of a predicted label in a test environment with a different sound speed profile than the training environment. Observe that the pre-trained model prediction (the label with maximum probability) is far from the ground truth, however, there is another peak in the output closer to the ground-truth.

peak in the output is not necessarily aligned with the true label. To decide which peak to select, we leverage another estimation process based on the received signal strength, which is potentially more robust and is only required to provide a coarse estimate. Note that array-based localization usually involves normalization by the total received signal power at the array elements, which is supposed to remove the source power information and make the algorithm robust to the source power. There are also methods that use the received signal strength for localization [19], [20]. We propose that combining these two approaches in a Bayesian manner can enhance the generalization performance.

## II. LOCALIZATION USING SAMPLE COVARIANCE MATRICES

**Notation:** Bold letters denote matrices and vectors,  $H(\mathbf{y})$  indicates the discrete entropy of the PMF  $\mathbf{y}$ ,  $D_{KL}$  denotes the KL-divergence,  $\mathcal{R}\{x\}$  and  $\mathcal{I}\{x\}$  respectively denote the real and imaginary parts of  $x$ ,  $\mathbf{A}^T$  and  $\mathbf{A}^H$  denote respectively the transpose and conjugate transpose of the matrix or vector  $\mathbf{A}$ . Also, for a set of test points  $\mathcal{S}$ , the complement is shown by  $\mathcal{S}^c = \mathcal{D}_{test} - \mathcal{S}$  and the cardinality is shown by  $|\mathcal{S}|$ .

Sample covariance matrices (SCM) are usually used for UWA localization using arrays because they are sufficient statistics for the jointly Gaussian signal and noise [21] scenarios. The normalized SCM of an  $L$  element array using  $P$  snapshots  $\tilde{\mathbf{R}}^{(p)}(f)$  is calculated as

$$\tilde{\mathbf{C}} = \frac{1}{P} \sum_{p=1}^P \tilde{\mathbf{R}}^{(p)}(f) \tilde{\mathbf{R}}^{(p)}(f)^H, \quad (1)$$

where  $\tilde{\mathbf{R}}^{(p)}(f) = [\tilde{R}_1^{(p)}(f), \tilde{R}_2^{(p)}(f), \dots, \tilde{R}_L^{(p)}(f)]^T$  and

$$\tilde{R}_l^{(p)}(f) = \frac{R_l^{(p)}(f)}{\sqrt{\sum_{l=1}^L |R_l^{(p)}(f)|^2}}, \quad l \in \{1, 2, \dots, L\}, \quad (2)$$

where the scalar  $R_l^{(p)}(f)$  is the complex Fourier coefficient of the  $p$ -th segment of the  $l$ -th hydrophone received signal at

the frequency  $f$ . We use a 3-second-long signal divided into  $P = 5$  segments, each of length 1 second and a 50% overlap, tapered by a Kaiser window with  $\beta = 9.24$ . The goal is to determine the source range  $d$ , given the corresponding SCM  $\tilde{\mathbf{C}}$ . Since we assume that the source signal is monotone at frequency  $f$ , we will drop  $f$  from the notation in the following sections.

### A. MFP approach

We use the Bartlett processor [22] as an MFP baseline, which is described by

$$\hat{d} = \arg \max_d \tilde{\mathbf{R}}(d)^H \tilde{\mathbf{C}} \tilde{\mathbf{R}}(d), \quad (3)$$

where  $\tilde{\mathbf{C}}$  is the normalized SCM of the measured data and  $\tilde{\mathbf{R}}(d)$  is the replica field generated by a source at range  $d$ . For each  $d$ , the corresponding  $\tilde{\mathbf{R}}(d)$  from the training set is used at the inference time. Observe that this method has access to training data at the test time, however, we do not adapt  $\tilde{\mathbf{R}}(d)$  to the new environment.

### B. CNN approach

As depicted in Fig. 3, the feature extractor part of the model is a CNN followed by a linear layer, that takes the real and imaginary parts of the SCM,  $[\mathcal{R}\{\tilde{\mathbf{C}}_i\} | \mathcal{I}\{\tilde{\mathbf{C}}_i\}]$ , as the 2-channel input (a real tensor of dimension  $2 \times L \times L$ ) and generates the feature vector  $\phi_i$ . These features are then fed into a linear classifier to generate the output PMF  $\hat{\mathbf{y}}_i$ . Denoting the area of interest for the source range by  $[D_{\min}, D_{\max}]$ , for each training sample  $i$ , we quantize the range  $d_i$  by  $d_i^q = \lfloor \frac{d_i - D_{\min}}{100} + 0.5 \rfloor$ . Although in classification tasks, usually a one-hot representation of  $d_i^q$  is used, since we use mean absolute error (MAE) to evaluate our results, we define the soft label  $\mathbf{y}_i = [y_{i1}, y_{i2}, \dots, y_{iM}] = \eta(d_i^q)$  as

$$y_{ik} = \frac{\exp(-|k - d_i^q|/\sigma)}{\sum_{k=1}^M \exp(-|k - d_i^q|/\sigma)}, \quad (4)$$

where,  $M$  is the number of classes and  $\sigma$  is a hyper-parameter. Figure 2 shows one such smoothed label.

Therefore, the training dataset is denoted by  $\mathcal{D}_{tr} = \{([\mathcal{R}\{\tilde{\mathbf{C}}_i\} | \mathcal{I}\{\tilde{\mathbf{C}}_i\}], \mathbf{y}_i)\}_{i=1}^{N_{tr}}$  and the test set that does not include labels is denoted by  $\mathcal{D}_{test} = \{([\mathcal{R}\{\tilde{\mathbf{C}}_i\} | \mathcal{I}\{\tilde{\mathbf{C}}_i\}]\}_{i=1}^{N_{test}}$ . We use the loss function  $\mathcal{L}_{tr} = \frac{1}{N_{tr}} \sum_{i=1}^{N_{tr}} \text{JSD}(\mathbf{y}_i, \hat{\mathbf{y}}_i)$  for training, where  $\hat{\mathbf{y}}_i$  is the network output and JSD is the specific Jensen-Shannon Divergence [23] defined by

$$\text{JSD}(\mathbf{y}_i, \hat{\mathbf{y}}_i) = \frac{1}{2} (D_{KL}(\mathbf{y}_i \| \bar{\mathbf{y}}_i) + D_{KL}(\hat{\mathbf{y}}_i \| \bar{\mathbf{y}}_i)), \quad (5)$$

where  $\bar{\mathbf{y}}_i = (\mathbf{y}_i + \hat{\mathbf{y}}_i)/2$ .

The CNN structure is similar to that in [2] with a 2 channel input, 3 convolutional layers with 6, 38, and 40 channels and kernels of size 3, 5, 5, respectively. The output of the feature extraction is a 256-dimensional vector  $\phi_i$ , which is then fed into the classifier to generate  $\hat{\mathbf{y}}_i$ .

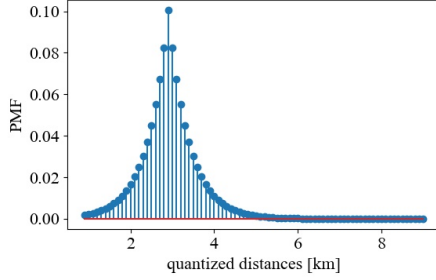


Fig. 2: An example of a metric-inspired smoothed label  $y_i$  corresponding to  $d_i^q = 20$ . Here, we have used the absolute error as the metric, hence, we have used a truncated exponential as the label.

### III. DOMAIN ADAPTATION

#### A. Environment Adaptation Using SHOT

When presented with data from a different environment, the network makes *uncertain* predictions, i.e., it will be confused between different classes, which leads to inaccurate predictions. However, since there is no labeled data from the new environment, we cannot supervise the model to make more accurate predictions. Nevertheless, we can encourage the model to preserve its predictions, with a higher confidence, on samples that match to the training data. To this end, we select a self-supervising subset  $\mathcal{S}$  of the samples and use the pre-trained network's output on these samples as their pseudo-labels, for which we use a loss term  $\text{JSD}(\mathbf{y}_i^{\text{pseudo}}, \hat{\mathbf{y}}_i)$ . Here,  $\mathbf{y}_i^{\text{pseudo}}$  is the softened labeled based on the output of the pre-trained classifier. However, to prevent the network from only predicting classes that exist in the self-supervising subset, for all of the samples, we add a loss term that seeks to maximize the entropy of the outputs average  $\bar{\mathbf{y}} = \frac{1}{N_{\text{test}}} \sum_{i=1}^{N_{\text{test}}} \hat{\mathbf{y}}_i$ .

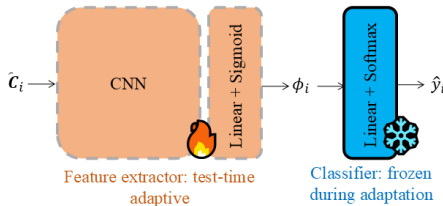


Fig. 3: The CNN classifier includes a feature extraction part followed by a linear classifier that will be frozen during adaptation.

To determine the self supervising set  $\mathcal{S}$ , first note that we freeze the pre-trained classifier as depicted in Fig. 3, which predicts the label  $\hat{\mathbf{y}}_i$  by

$$\hat{\mathbf{y}}_i = \text{Softmax}(\mathbf{w}_k^T \phi_i), \quad (6)$$

where  $\mathbf{w}_k$  is the classification weight vector corresponding to the  $k$ -th class. Note that if the feature vector  $\phi_i$  is highly aligned with  $\mathbf{w}_{k_0}$  for one  $k_0$ , then the network predicts a unimodal soft label  $\hat{\mathbf{y}}_i$ , as opposed to situations where the

network generates a multimodal output and is not certain about the predicted label. Inspired by this observation, we construct the self-supervising subset  $\mathcal{S}$  according to

$$\mathcal{S} = \{i : 1 \leq i \leq N_{\text{test}} \text{ s.t. } \hat{\mathbf{y}}_i \text{ has only 1 significant peak}\}, \quad (7)$$

where a significant peak is either the only peak or it is more than 10 times larger than the second largest peak.

To perform source hypothesis, we define the SHOT loss by

$$\mathcal{L}_{\text{SHOT}} = -H(\bar{\mathbf{y}}) + \frac{\beta}{|\mathcal{S}|} \sum_{i \in \mathcal{S}} \text{JSD}(\mathbf{y}_i^{\text{pseudo}}, \hat{\mathbf{y}}_i), \quad (8)$$

where,  $\beta$  is a positive weight. We then employ the Adam optimizer [24] to minimize  $\mathcal{L}_{\text{SHOT}}$  with a learning rate of  $\mu_{DA}$ . This loss encourages the network to adapt itself in a way to be more certain about its predictions, while preventing it from assigning all inputs to the same output by encouraging diverse outputs [9]. This approach is effective for rectifying errors due to small mismatches.

#### B. Joint Source-Environment Adaptation (JSEA)

Given that  $\mathbf{C} = E \tilde{\mathbf{C}}$ , where  $E = \sum_{l=1}^L |R_l^{(p)}(f)|^2$  (which is accurate for  $P = 1$  snapshot case and approximately correct for  $P > 1$ ), and assuming that  $E$  and  $\tilde{\mathbf{C}}$  are independent,

$$\begin{aligned} p(\mathbf{y}|\mathbf{C}) &= p(\mathbf{y}|\tilde{\mathbf{C}}, E) = \frac{p(\tilde{\mathbf{C}}, E|\mathbf{y})p(\mathbf{y})}{p(\tilde{\mathbf{C}})p(E)} \\ &= \frac{p(\tilde{\mathbf{C}}|E, \mathbf{y})p(E|\mathbf{y})p(\mathbf{y})}{p(\tilde{\mathbf{C}})p(E)} = \frac{p(\mathbf{y}|\tilde{\mathbf{C}})p(\mathbf{y}|E)}{p(\mathbf{y})}. \end{aligned} \quad (9)$$

As a result, if  $\mathbf{y}$  is uniformly distributed over the area of interest, we have  $p(\mathbf{y}|\mathbf{C}) \propto p(\mathbf{y}|\tilde{\mathbf{C}})p(\mathbf{y}|E)$ .  $E$  depends on the source power that can be estimated from  $\mathcal{S}$  in (7). Note that both  $p(\mathbf{y}|\tilde{\mathbf{C}})$  and  $p(\mathbf{y}|E)$  can be used for localization. However,  $p(\mathbf{y}|\tilde{\mathbf{C}})$  provides a finer estimate (and typically more sensitive to mismatches), while  $p(\mathbf{y}|E)$  provides a coarser estimate that is more robust to environmental mismatches. Therefore, by exploiting both terms we can significantly improve the performance of localization algorithms in the presence of mismatches.

To achieve  $p(\mathbf{y}|E)$ , we assume that  $E|d \sim \mathcal{N}(\Gamma_s(d), \sigma_s^2)$ , where  $\Gamma_s$  (transmission loss) is a source-environment dependent decreasing function of  $d$ , and  $\sigma_s$  is an environmental dependent hyper-parameter. Note that although this assumption is not accurate (since  $E \geq 0$ ), the result is still useful for our purpose. For simplicity, we assume  $\Gamma$  is piece-wise constant, hence, can be estimated from the self-supervised samples by  $\hat{\Gamma}_\delta(d) = \frac{1}{|\mathcal{S}_\delta(d)|} \sum_{k \in \mathcal{S}_\delta(d)} E_k$ , where  $\mathcal{S}_\delta(d) = \{k \in \mathcal{S}; |d - \hat{d}_k| \leq \delta\}$ , and  $E_k$  is the received energy of the  $k$ -th sample. Then for each  $i \in \mathcal{S}^c$  and  $k = 1, \dots, M$ ,  $p(E_i|d_k^q) \propto \exp(-\frac{|E_i - \hat{\Gamma}_\delta(d_k^q)|^2}{2\sigma_s^2})$ , which can be then converted to  $p(\mathbf{y}|E)$  using  $p(E_i) = \sum_{\mathbf{y}} p(E_i|\mathbf{y})p(\mathbf{y})$  and  $p(\mathbf{y}) = 1/M$ .

However, since we only need a coarse estimate from the source adaptation part, to rely more on the neural network for

the finer estimation, we obtain the pseudo label by  $\mathbf{y}_i^{\text{pseudo}} = \eta(d_{k^*}^q)$ , where

$$k^* = \arg \min_{k \in \mathcal{P}(i)} |E_i - \hat{\Gamma}_\delta(d_k^q)|, \quad (10)$$

and  $\mathcal{P}(i)$  denotes the set of output peaks for sample  $i$ . Having defined the pseudo-labels for both  $\mathcal{S}$  and  $\mathcal{S}^c$ , we finally adapt the feature extractor using the JSEA loss defined by

$$\mathcal{L}_{\text{JSEA}} = \sum_{i=1}^{N_{\text{test}}} \text{JSD}(\mathbf{y}_i^{\text{pseudo}}, \hat{\mathbf{y}}_i). \quad (11)$$

#### IV. EMPIRICAL EVALUATION

We generate data using Bellhop [25], where the environmental parameters are set according to the SWellEx-96 [3], [22] experiment. As depicted in Fig. 4, the training data consist of source ranges between 900 m and 9 km with 10 m increments (thus, 811 distinct samples), and a 21-element vertical linear array (VLA) placed at depths from 94.125 m to 212.25 m to mimic the SWellEx-96 data. Moreover, the source depth is 54 m and it transmits a monotone signal with frequency  $f = 130$  Hz. Note that we have considered a single-layered bottom with a flat bathymetry at depth 216 m in our simulations and used the average sound speed profile from the SWellEx-96 measurements.

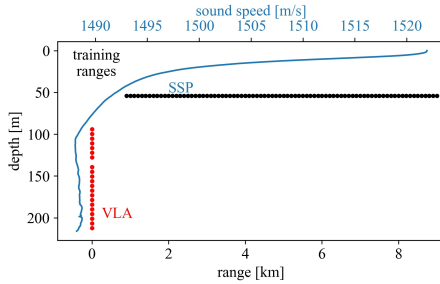


Fig. 4: Bellhop environment inspired by the SWellEx-96.

To generate a test environment that has a sound speed  $c(z)$  at depth  $z$ , slightly different from that of the training environment,  $c_0(z)$ , we use a constant gradient perturbation as  $c(z) = c_0(z) + \frac{\Delta c}{215}(z - 215)$ , where  $0 \leq z \leq 215$ . We generate data according to random source ranges between  $D_{\min} = 900$  m and  $D_{\max} = 9$  km, and divide the region into 100 m-long intervals, each represented by its mid point. Consequently, the labels and classifier outputs are  $M = 82$  dimensional. In addition to emulating the real ocean environment in the test time, we add a randomly selected noise segment  $w$  from the KAM11 experiment [26] (scaled to have a desired noise power) to the generated signal for each hydrophone. Accordingly, we use the average array SNR, defined as

$$\text{SNR [dB]} = 10 \log_{10} \frac{\sum_{l=1}^L E_l}{L E_w},$$

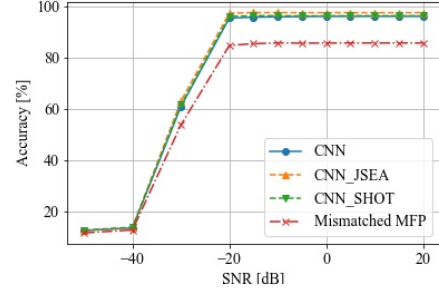
where  $E_l = |R_l|^2$  is the energy of the received signal at the  $l$ -th hydrophone and  $E_w$  is the noise power spectral density at the frequency  $f = 130$  Hz.

We evaluate models based on MAE and probability of credible localization (PCL) defined as

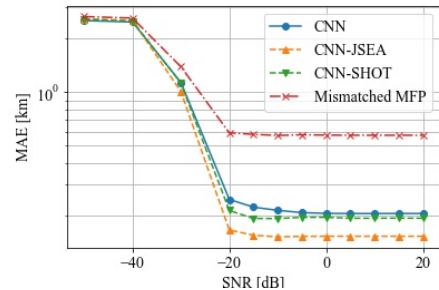
$$\text{PCL} = 100 \times \frac{\sum_{i=1}^{N_{\text{test}}} \mathbf{1}_{|d_i - \hat{d}_i| \leq 0.1 d_i}}{N_{\text{test}}},$$

where  $d_i$  is the true distance of the  $i$ -th sample and  $\hat{d}_i = 100 \arg \max \hat{\mathbf{y}}_i + D_{\min}$  is the estimated distance. To train the network, we use  $\sigma = 5$  for label softening, a learning rate of  $10^{-4}$  for the Adam optimizer, and a batch size of 128. Furthermore, we randomly split the data into 85% training and 15% validation sets. Also, to prevent over-fitting, we multiply the learning rate by 0.1 whenever there is no reduction in the validation error after 75 iterations, and we stop training if there is no reduction in the validation error after 125 iterations. The results are averaged over 100 noise realizations.

The CNN-SHOT uses (8) for adaptation, while CNN-JSEA uses (11). For both adaptation methods, we use  $\mu_{DA} = 5 \times 10^{-6}$ , and  $\beta = 1$  in (8) and we use  $\delta = 500$  m in (10). Figure 5 shows the superiority of the JSEA method when the only difference between the training and testing environments is noise. In addition, according to Figs. 6a and 6b, a small perturbation in the sound speed profile (along with mismatch in noise statistics) results in a significant mismatch in the arrival structure, as the MFP's performance deteriorates quickly. Nevertheless, JSEA can significantly enhance the MAE and PCL of the CNN.

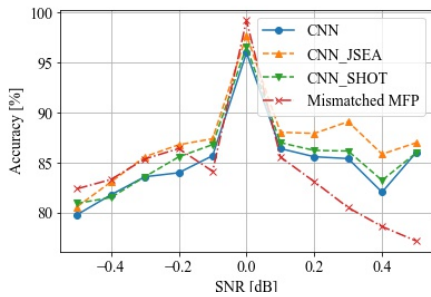


(a) PCL

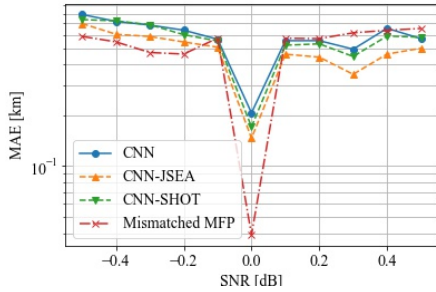


(b) MAE

Fig. 5: Performance under different SNR values, with KAM11 noise and  $\Delta c = 0.1$  m/s.



(a) PCL under small mismatch in SSP.



(b) MAE under small mismatch in SSP.

Fig. 6: Performance under different amounts of SSP mismatch at an SNR of 0 dB. Observe the sharp deterioration of the MFP performance for the small mismatches.

## V. CONCLUSION

By using classification for localization, the model outputs reveal the confident samples that we use to make an estimation based on the source power. We use this estimation to generate pseudo-labels for uncertain samples. We showed that while SHOT can slightly improve the performance by encouraging the network to make its predictions less uncertain on the samples similar to the training set, JSEA can significantly improve the UWA localization that almost always suffers in the presence of environmental mismatch. With more prior knowledge about domain shifts between the training and testing environments and source location distribution, one may be able to improve performance using more effective methods for selecting  $S$  even without access to training data. However, the performance improvement will be limited in the absence of such knowledge.

## REFERENCES

- [1] H. Niu, E. Reeves, and P. Gerstoft, "Source localization in an ocean waveguide using supervised machine learning," *The Journal of the Acoustical Society of America*, vol. 142, no. 3, pp. 1176–1188, 2017.
- [2] R. Chen and H. Schmidt, "Model-based convolutional neural network approach to underwater source-range estimation," *The Journal of the Acoustical Society of America*, vol. 149, no. 1, pp. 405–420, 2021.
- [3] Y. Wang and H. Peng, "Underwater acoustic source localization using generalized regression neural network," *The Journal of the Acoustical Society of America*, vol. 143, no. 4, pp. 2321–2331, 2018.
- [4] Y. Liu, H. Niu, Z. Li, and D. Zhai, "Unsupervised domain adaptation for source localization using ships of opportunity with a deep vertical line array," *IEEE Journal of Oceanic Engineering*, 2023.

- [5] Y. Ganin and V. Lempitsky, "Unsupervised domain adaptation by back-propagation," in *International conference on machine learning*. PMLR, 2015, pp. 1180–1189.
- [6] Y. Song, "Underwater acoustic sensor networks with cost efficiency for internet of underwater things," *IEEE Transactions on Industrial Electronics*, vol. 68, no. 2, pp. 1707–1716, 2020.
- [7] X. Zhuo, M. Liu, Y. Wei, G. Yu, F. Qu, and R. Sun, "Auv-aided energy-efficient data collection in underwater acoustic sensor networks," *IEEE Internet of Things Journal*, vol. 7, no. 10, pp. 10010–10022, 2020.
- [8] W. Zhang, G. Han, X. Wang, M. Guizani, K. Fan, and L. Shu, "A node location algorithm based on node movement prediction in underwater acoustic sensor networks," *IEEE Transactions on Vehicular Technology*, vol. 69, no. 3, pp. 3166–3178, 2020.
- [9] J. Liang, D. Hu, and J. Feng, "Do we really need to access the source data? source hypothesis transfer for unsupervised domain adaptation," in *International conference on machine learning*. PMLR, 2020, pp. 6028–6039.
- [10] A. B. Baggeroer, W. Kuperman, and H. Schmidt, "Matched field processing: Source localization in correlated noise as an optimum parameter estimation problem," *The Journal of the Acoustical Society of America*, vol. 83, no. 2, pp. 571–587, 1988.
- [11] E. J. Sullivan and D. Middleton, "Estimation and detection issues in matched-field processing," *IEEE journal of oceanic engineering*, vol. 18, no. 3, pp. 156–167, 1993.
- [12] H. Schmidt, "Ocean acoustics and seismic exploration synthesis (oases)," 2012.
- [13] K. Zhang, B. Schölkopf, K. Muandet, and Z. Wang, "Domain adaptation under target and conditional shift," in *International conference on machine learning*. PMLR, 2013, pp. 819–827.
- [14] W. Wang, H. Ni, L. Su, T. Hu, Q. Ren, P. Gerstoft, and L. Ma, "Deep transfer learning for source ranging: Deep-sea experiment results," *The Journal of the Acoustical Society of America*, vol. 146, no. 4, pp. EL317–EL322, 2019.
- [15] J. Yosinski, J. Clune, Y. Bengio, and H. Lipson, "How transferable are features in deep neural networks?" *Advances in neural information processing systems*, vol. 27, 2014.
- [16] H. Yao, Y. Wang, S. Li, L. Zhang, W. Liang, J. Zou, and C. Finn, "Improving out-of-distribution robustness via selective augmentation," in *International Conference on Machine Learning*. PMLR, 2022, pp. 25 407–25 437.
- [17] Y. Liu, H. Niu, Z. Li, and M. Wang, "Deep-learning source localization using autocorrelation functions from a single hydrophone in deep ocean," *JASA Express Letters*, vol. 1, no. 3, 2021.
- [18] R. Long, J. Zhou, N. Liang, Y. Yang, and H. Shen, "Deep unsupervised adversarial domain adaptation for underwater source range estimation," *The Journal of the Acoustical Society of America*, vol. 154, no. 5, pp. 3125–3144, 2023.
- [19] T. Xu, Y. Hu, B. Zhang, and G. Leus, "Rss-based sensor localization in underwater acoustic sensor networks," in *2016 IEEE International Conference on Acoustics, Speech and Signal Processing (ICASSP)*. IEEE, 2016, pp. 3906–3910.
- [20] B. Zhang, H. Wang, T. Xu, L. Zheng, and Q. Yang, "Received signal strength-based underwater acoustic localization considering stratification effect," in *OCEANS 2016 - Shanghai*, 2016, pp. 1–8.
- [21] P. Gerstoft, H. Groll, and C. F. Mecklenbräuker, "Parametric bootstrapping of array data with a generative adversarial network," in *2020 IEEE 11th Sensor Array and Multichannel Signal Processing Workshop (SAM)*. IEEE, 2020, pp. 1–5.
- [22] K. L. Gemba, W. S. Hodgkiss, and P. Gerstoft, "Adaptive and compressive matched field processing," *The Journal of the Acoustical Society of America*, vol. 141, no. 1, pp. 92–103, 2017.
- [23] B. Fuglede and F. Topsøe, "Jensen-shannon divergence and hilbert space embedding," in *International symposium on Information theory, 2004. ISIT 2004. Proceedings*. IEEE, 2004, p. 31.
- [24] D. P. Kingma and J. Ba, "Adam: A method for stochastic optimization," in *ICLR (Poster)*, 2015. [Online]. Available: <http://arxiv.org/abs/1412.6980>
- [25] M. B. Porter, "The bellhop manual and user's guide: Preliminary draft," *Heat, Light, and Sound Research, Inc., La Jolla, CA, USA, Tech. Rep.*, vol. 260, 2011.
- [26] B. Tomasi, J. Preisig, and M. Zorzi, "On the predictability of underwater acoustic communications performance: The KAM11 data set as a case study," in *Proceedings of the 6th International Workshop on Underwater Networks*, 2011, pp. 1–7.